NANOPARTICLES FROM COMPOUNDS WITH LAYERED STRUCTURES

D. VOLLATH† and D. V. SZABÓ

Forschungszentrum Karlsruhe, Institut fur Materialforschung III, PO Box 3640, D 76021 Karlsruhe, Germany

Abstract Layered structures of the type B8, C6, and C7 excel in the fact that the binding within the layers between the metal and the non metal is of the covalent type and between the layers of the van der Waals type. This leads, in the case of nanoparticles, to a large number of dangling bonds on the periphery of the layers. In the well studied case of graphite, the formation of onion like structures and nanotubes reduces the free energy of the system. It is shown that the formation of these morphologies is very general for small particles. This is shown for BN, MoS_2, WS_2, WSe_2, and $MoSe_2$. SnS_2 and $ZrSe_2$ are special exceptions, as nanoparticles of these compounds preferably form rope like structures. These experiments lead to the general rule that nanoparticles made of layered compounds try to form closed structures.

Keywords: Layered structures; Nitrides

1. INTRODUCTION

Nanoparticles of compounds with layered structure are of special interest because some of them may form fullerenes, nested fullerene like structures, or tubes. The nested fullerene like structures are also known as "onion crystals". This phenomenon was found originally in the case of carbon. In the mean time, similar phenomena were found in a few other compounds. The first nested fullerene like structures in non carbon compounds were found in WS_2 [1], MoS_2 [2, 3] films on quartz substrates and in BN particles [4]. The sulphides [1, 2] were obtained by the reaction of the metal films with H_2S at a temperature of 1000°C. The synthesis of MoS_2 powder by the reaction of MoO_3 with H_2S in a hydrogen containing atmosphere at a temperature above 650°C yields MoS_2 particles with sizes in the range of 50 100 nm. Additionally, onion crystals with diameters up to 30 nm and nanotubes with length up to a few micrometres were found [5]. Interestingly, nested structures have been shown also in MoS_2 produced by laser ablation by Parilla *et al*. [6]. BN particles with sizes in the range from 20 to 100 nm crystallizing in plate like and concentric shell shapes were synthesized by a laser induced reaction between BCl_3 and NH_3 [4, 7, 8].

This knowledge leads to the question of whether this is a general phenomenon found in layered structures. In this context, the dependency of the formation of these particles on the particle size is also open. To find a first answer to these questions, nanoparticles of compounds crystallizing in three different types of layered structure were synthesized and analysed. The layered structures selected for this study are hexagonal ones excelling in the fact that the binding within the layers between the metal and the non metal is of the covalent type and between the hexagonal layers of the van der Waals type. This is why some of these compounds may be used as lubricants. Because of the relatively weak van der Waals binding between the planes, varying distances in the *c* direction are found, whereas the distances in the *a* direction are always close to the values found in coarse material. The varying *c* values depend strongly on the conditions of synthesis [5]. In most cases, the lattice is expanded in the *c* direction [1, 2, 5, 6]. For closed shells, this dilation is smaller [9], and in a few cases a contraction was observed [10].

In the framework of this study the following structures were selected:

B8 (NiAs) type structure. This structure consists of hexagonal planes each with the exact stoichiometric ratio Me/X 1 of the metal ions Me and the non metal ions X. The stacking sequence is ... A B A B .... The material selected for demonstration was BN.

† To whom all correspondence should be addressed.

C6 (PbJ_2) type structure. In this structure the layers consist of three planes: one hexagonal plane consisting of the metal ions, Me, is placed between two hexagonal planes consisting of the non metal ions, X. Therefore, the sequence of the planes in these layers is ...X Me X X Me X.... The stacking sequence of the planes is ... BCA BCA BCA .... As examples for this group, $ZrSe_2$ and SnS_2 were selected.

C7 (MoS_2) type structure. Similar to the C6 case, in this structure the layers consist of three planes: one hexagonal plane consisting of the metal ions, Me, placed between two hexagonal planes consisting of the non metal ions, X. Again, the sequence of the planes in these layers is ...X Me X X Me X... whereas the stacking sequence of the layers is ... BAB ABA BAB .... As examples for this group the sulphides and selenides of molybdenum and tungsten were selected.

The microwave plasma process, originally developed for the synthesis of oxide and nitride nanoparticles, was used to synthesize the specimen [11, 12].

2. EXPERIMENTAL

2.1. Synthesis

The synthesis was performed in a microwave plasma, using microwaves with a frequency of 0.915 or 2.45 GHz [13]. In both cases the plasma reaction is performed in a quartz tube passing a monomode microwave cavity [14]. The precursor compounds were vaporized outside of the reaction zone and introduced to the reaction gas in front of the plasma zone, where the nanoparticles are formed. The reaction gas was preheated to avoid precipitation of the precursor compounds. Using a 0.915 GHz plasma, the reaction was performed under a pressure of 30 mbar. The reaction temperature was adjusted at 260 or 580°C. The flow rate of the gas was adjusted to obtain a residence time of the particles of about 8 ms in the reaction zone at a temperature of 580°C and about 4 ms at 260°C. Using 2.45 GHz microwaves allows a further reduction of the reaction temperature. In this case it was possible to perform the reaction at a temperature as low as 160°C. The gas pressure was set to 10 mbar. This resulted in a residence time of the particles in the reaction zone of about 2 ms. In all cases, the reaction temperature was determined directly after the reaction zone. As a microwave plasma is a non equilibrium system, the true temperature of the particles during the formation was certainly different. In all cases, the reaction product was collected on cooled surfaces.

The following chemical routes were selected for the synthesis:

- Boron nitride, BN: To synthesize boron nitride, BCl_3 and a gas mixture of nitrogen with 4 vol.% H_2 was used.
- Sulphides: For the synthesis of the sulphides, H_2S was used as carrier for the sulphur. The plasma gas was a mixture of argon with 1 vol.% H_2S. The metals were introduced either as chloride ($SnCl_4$) or as carbonyl [$Mo(CO)_6$, $W(CO)_6$]. The reaction product consisted, besides the intended compound, of some elemental sulphur. To evaporate the free sulphur, the reaction product was heated up to a temperature of 120°C, respectively, 140°C in vacuum.
- Selenides: To obtain selenides, argon with 4 vol.% H_2 was used as plasma gas. Selenium was added as $SeCl_4$. This chloride was mechanically mixed in the proper stoichiometric ratio with the chloride of the metal in question. Fine particles of selenides are extremely sensitive against humid air. Therefore, the specimens for electron microscopy were collected under pure argon and as far as possible transferred under argon to the electron microscope.

2.2. Characterization

High resolution electron microscopy (Philips CM 30 ST) was applied for the morphological characterization of the reaction products. The preparation of the specimen for electron microscopy was made by two different methods.

- For a survey of the material carbon coated Cu grids were immersed in the reaction products. In this case, agglomerates consisting of a large number of particles are found on the grid.
- To study the morphology of individual particles it is necessary to have individual particles on the carbon coated grid. This was obtained by dispersing the reaction products ultrasonically in ethanol and dropping this dispersion on to the grids.

To analyse spacing and relative orientation of the lattice fringes, the electron micrographs were digitized and transformed in the Fourier space [15, 16]. Additionally, lattice distortions are seen easily by the shape of the maxima in the Fourier space. For reasons of simplicity, the power spectrum, the squared modulus of the Fourier transform, was applied for the evaluation of the images.

In the case of fullerene like and polyhedron shaped particles one has the additional problem of analysing this material in three dimensions. In the case of larger particles, the three dimensional structure can be shown by tilting the specimen in the transmission electron microscope. This is no longer feasible for particles with sizes below about 20 nm. In these cases, a series of micrographs with different defocus values was taken to obtain micrographs showing different parts of the particles under var

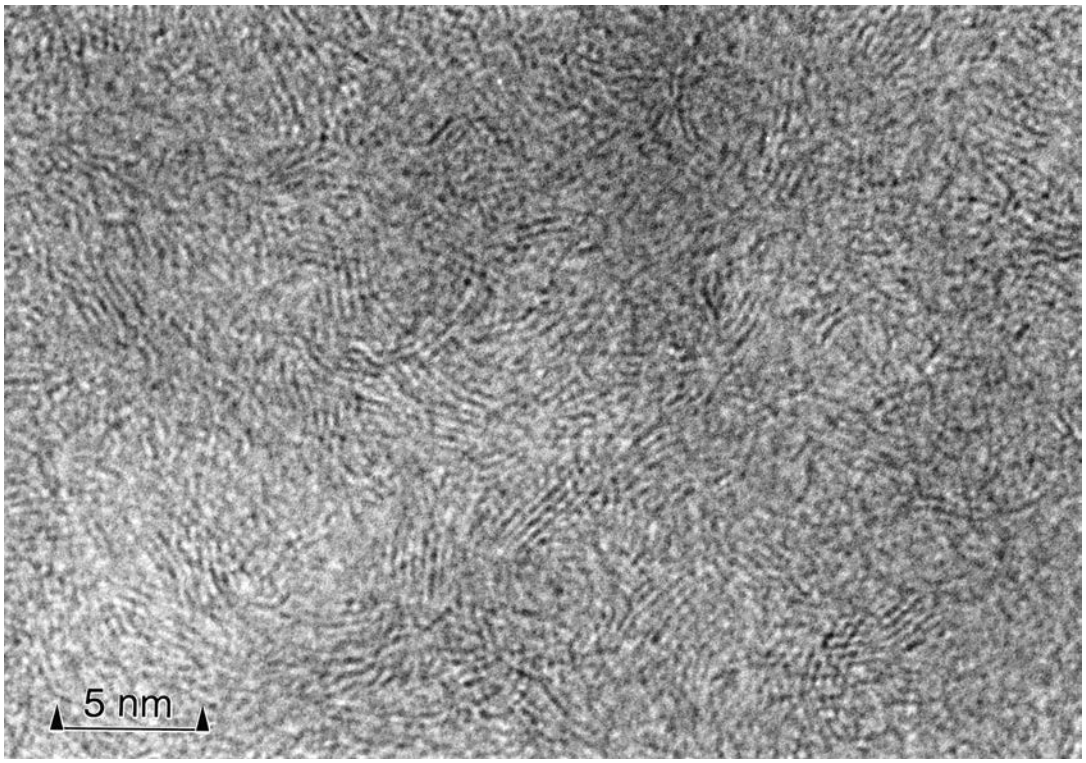

Fig. 1. Typical morphology of BN particles. One realizes a reduction of dangling bonds on the end of the planes by closing with other particles.

ious focus conditions. This technique provided ad ditional information about lattice orientation and distortion in different parts of the particles.

3. MORPHOLOGY OF THE PRODUCTS

3.1. Compounds with B8 structure, boron nitride, BN

Under the selected experimental conditions, BM forms particles with sizes in the range from 20 to 30 nm. Hexagonal BN is identified by electron dif fraction. BN particles form clusters of small pri mary particles. They appear ''sintered'' together, forming ''polycrystalline'' particles (Fig. 1). This ''sintering'' may rather be a closing of the dangling bonds of the small particles than the process that is usually understood with this term. It is interesting to note that Boulanger *et al.* [4] found a different type of closing dangling bonds by the formation of caps between the open ends of the lattice planes. In the primary particles analysed in this study, the lat tice planes are bent irregularly. Notably, some of these particles contain step dislocations. The lattice fringes in Fig. 1 show a spacing of 0.33 nm, corre sponding to the {0002} planes of the hexagonal BN (JCPDS value 0.33281 nm [17]). Hollow particles as described by Boulanger *et al.* [4] and Golberg *et al.* [18] were not found.

3.2. Compounds with C6 structure, $ZrSe_2$ and SnS_2

Small particles of these compounds generally show a filament like morphology. Figure 2 depict ing $ZrSe_2$ shows a characteristic example of these filaments. These filaments are arbitrarily bent and knotted together. At larger magnifications (Fig. 3) one realizes that the lattice planes show the same bends and twists as the particles. The lattice fringes in this micrograph represent the Se Zr Se {0002} layers with a distance of 0.36 nm (JCPDS value 0.3095 nm [19]). This filament like structure is not unique for $ZrSe_2$. It appears also in the case of SnS_2, as shown in Fig. 4, a typical micrograph. The distance of the lattice fringes for SnS_2 is 0.56 nm, corresponding with the {0001} planes (JCPDS value 0.589 nm [20]). Compared with $ZrSe_2$, the main difference is the smaller number of dislocation like structures. In addition to these filament like struc tures $ZrSe_2$ exhibited onion like crystal structures with varying distances between the lattice planes. An example is depicted in Fig. 5. In this case the distance between the lattice fringes was determined to be 0.34 nm. Similar onions were described by José Yacamán *et al.* [3] in the case of MoS_2 and Banhart *et al.* [10] in the case of carbon. In these two cases, varying distances between the lattice planes were also found. The lattice images (Figs 3 and 5) show layered structures, containing defects and varying distances between the planes. $ZrSe_2$

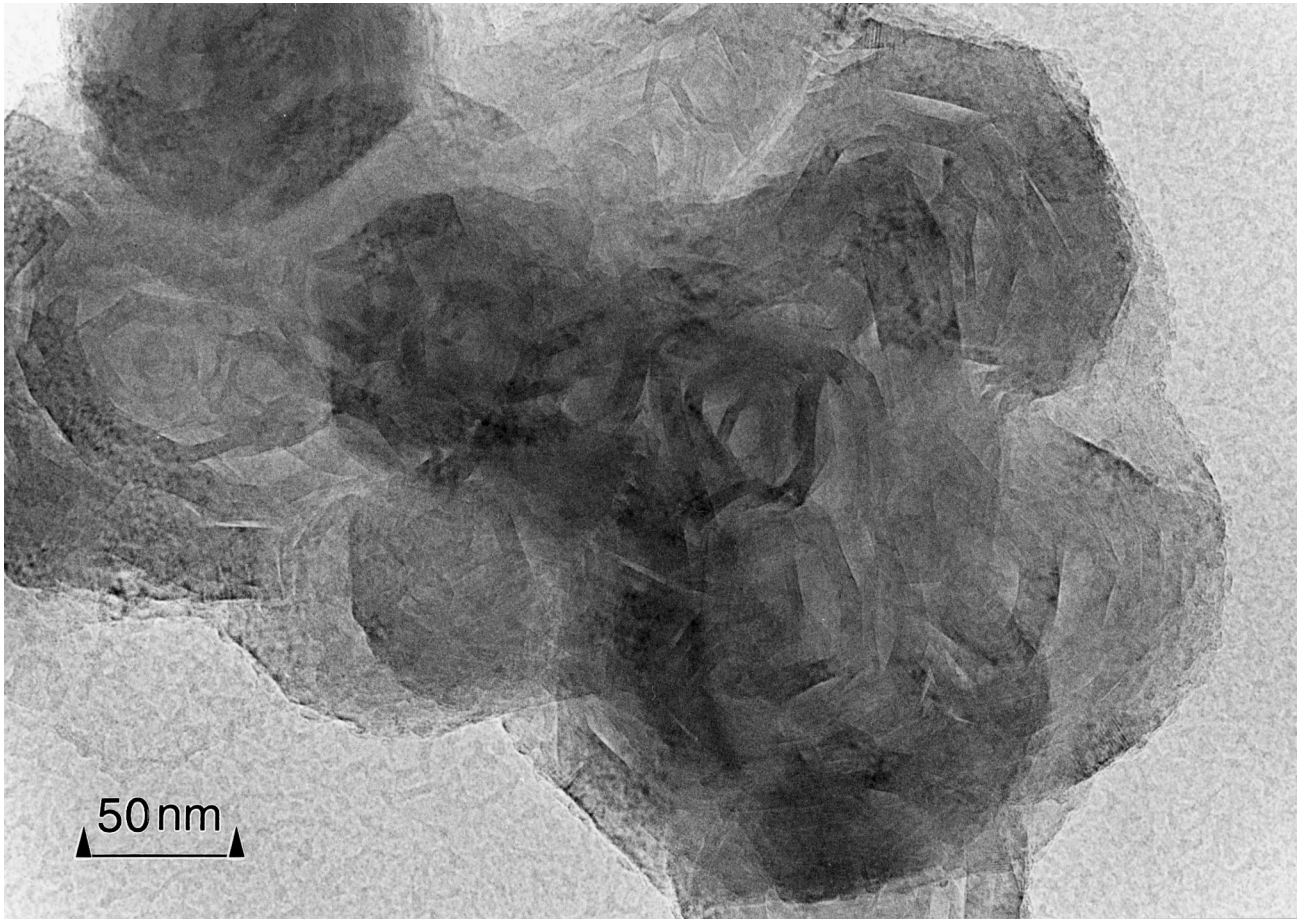

Fig. 2. Typical filament-like morphology found in zirconium selenide particles. The particles were synthesized in the 2.45 GHz equipment at 300°C.

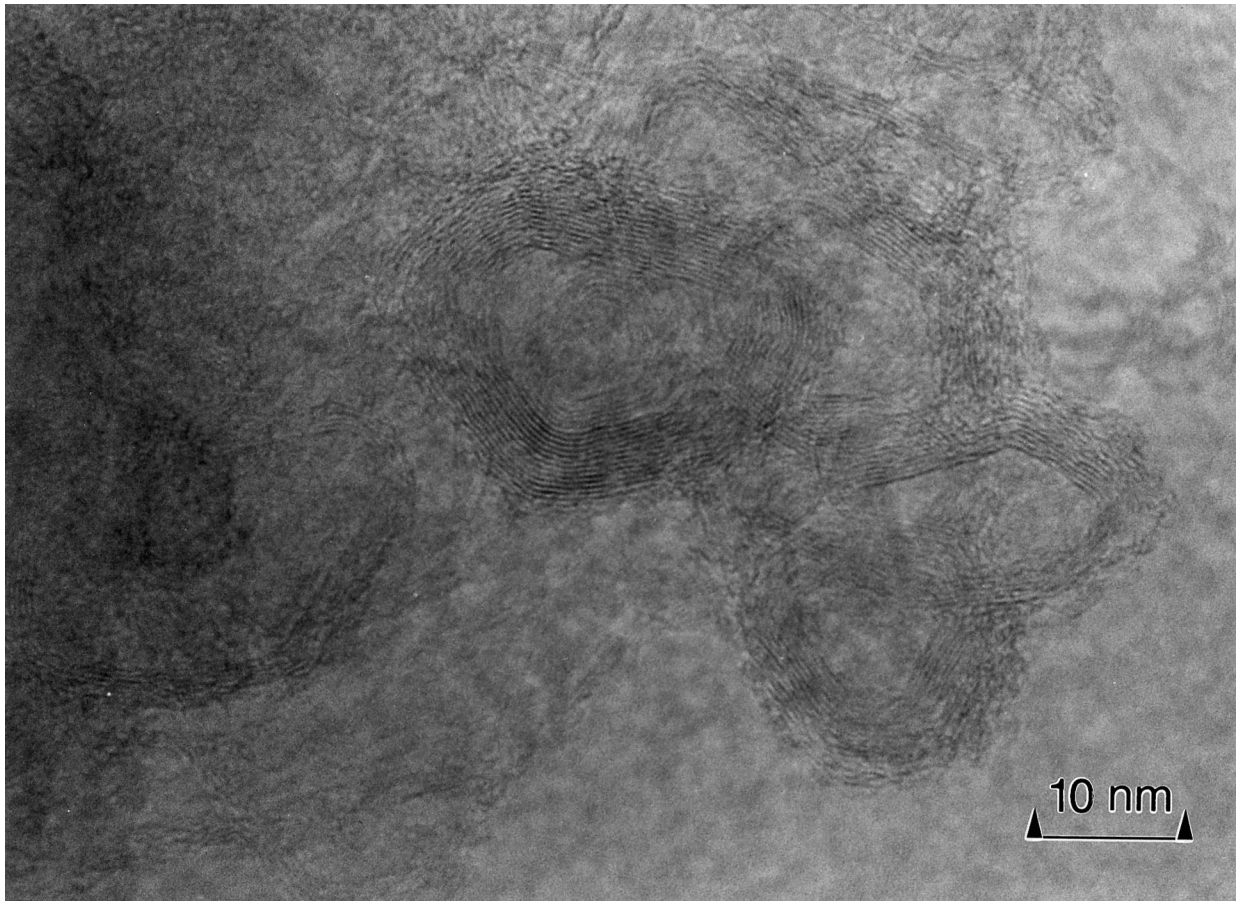

Fig. 3. Filament-like morphology of zirconium selenide particles at higher magnification. The distance of the lattice fringes is 0.36 nm. The structures are closed.

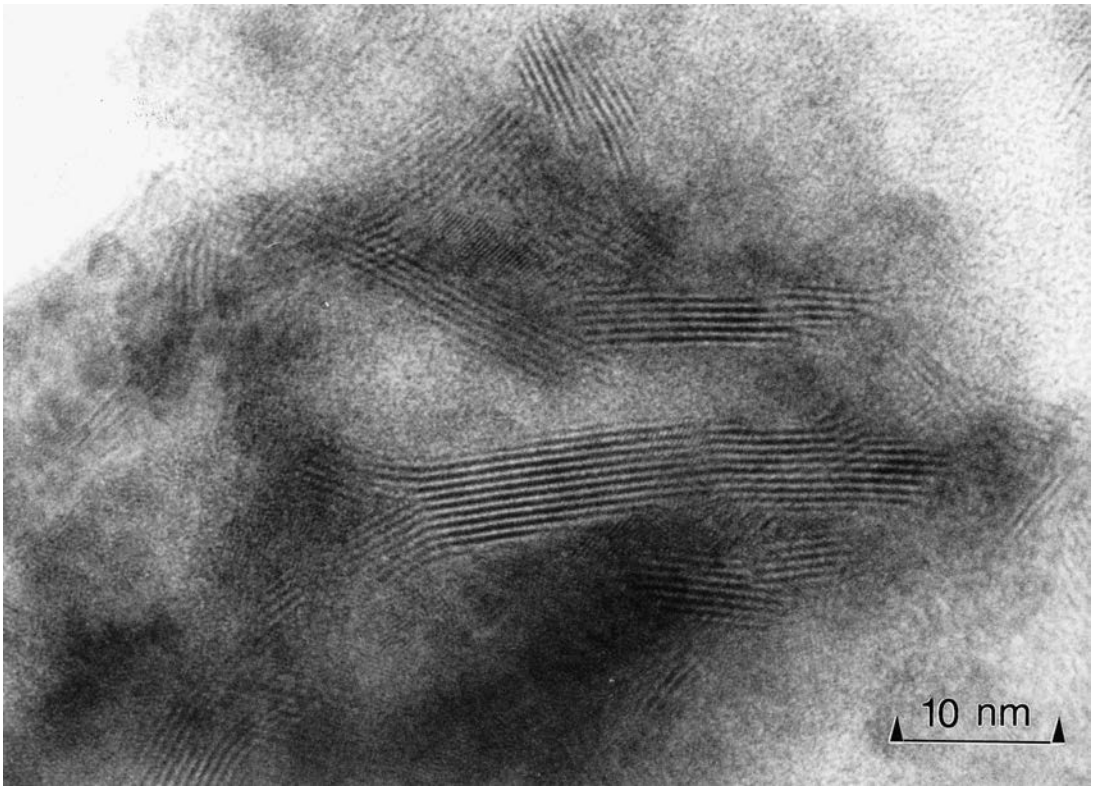

Fig. 4. Filaments of SnS_2, synthesized at 200°C. The filaments have a length of around 30 nm and a width of 3 5 nm. The distance between the lattice fringes is 0.56 nm which corresponds to the {0002} planes.

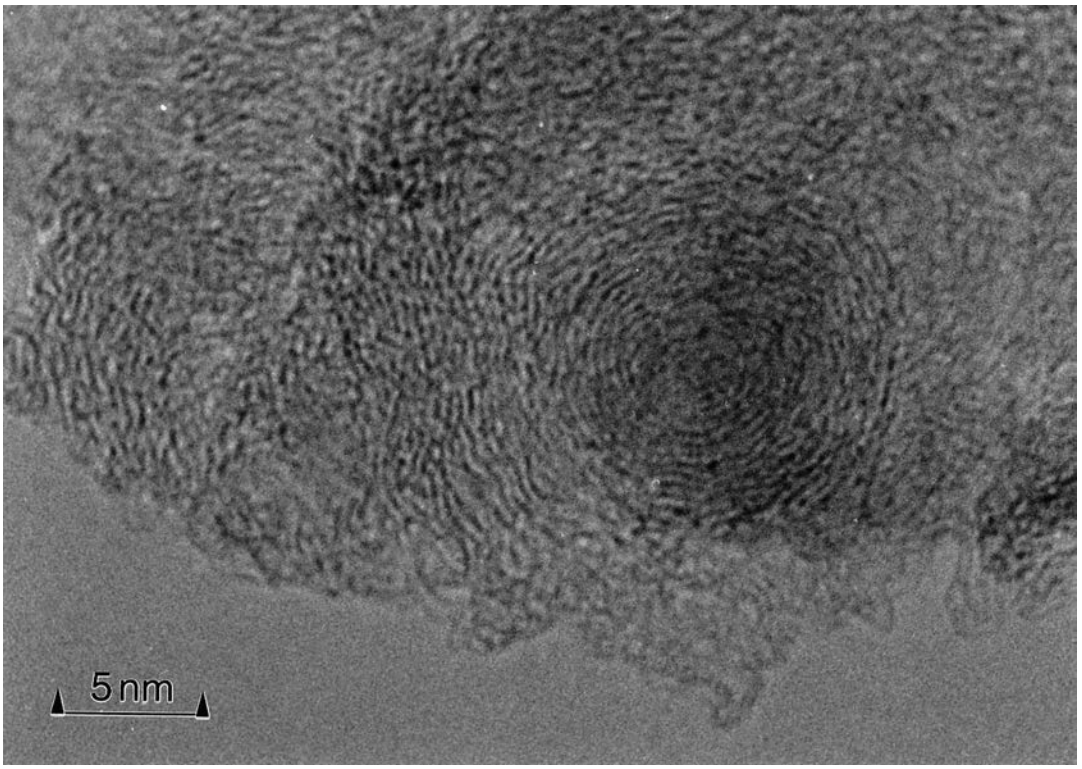

Fig. 5. Onion like zirconium selenide particle formed under observation of the filament like particles in the electron microscope.

Table 1. Results of the diffraction pattern evaluation of zinc sulphide, ZnS_2

Electron diffraction		β-SnS_2 JCPDS data #23-677 [20]			SnS_2 JCPDS data #21-1231 [21]		
d-values (nm)	Intensity	*hkl*	*d*-values (nm)	Intensity (%)	*hkl*	*d*-values (nm)	Intensity (%)
0.60	very strong	001	0.589	100	002	0.59	6
0.32	strong	100	0.3162	30	100	0.316	25
0.31	strong				101	0.305	16
		002	0.2951	5	004	0.294	10
0.28	weak	101	0.2784	55	102	0.278	45
					103	0.246	2
0.21	weak	102	0.215	25	104	0.215	4
		003	0.19665	5	006	0.196	< 2
		110	0.1824	30	110	0.182	100
0.175	weak	111	0.17431	20	112	0.174	20
0.169	weak	103	0.16693	8	106	0.166	< 2
		200	0.15801	4	200	0.158	25
					201	0.156	6
		112	0.15521	4	114	0.0155	2
		201	0.15263	8	202	0.152	10
0.148	weak	004	0.14749	4	008	0.145	< 2
		202	0.13928	5	204	0.139	4
0.115	weak	114	0.11469	7	118	0.115	

tends to recrystallize in the electron microscope. Therefore, it cannot be completely ruled out that the particles depicted are crystallized under the elec tron beam of the microscope.

The electron diffraction pattern obtained from the SnS_2 samples shows a pattern similar to both SnS_2 structures [20, 21] with a small expansion of 1.5% from 0.589 to 0.598 nm for the {0001} spa cing, whereas the lattice parameter in the *a* direc tion exhibits no expansion. Table 1 compares the diffraction patterns for the two SnS_2 phases accord ing to the JPCDS tables together with the exper

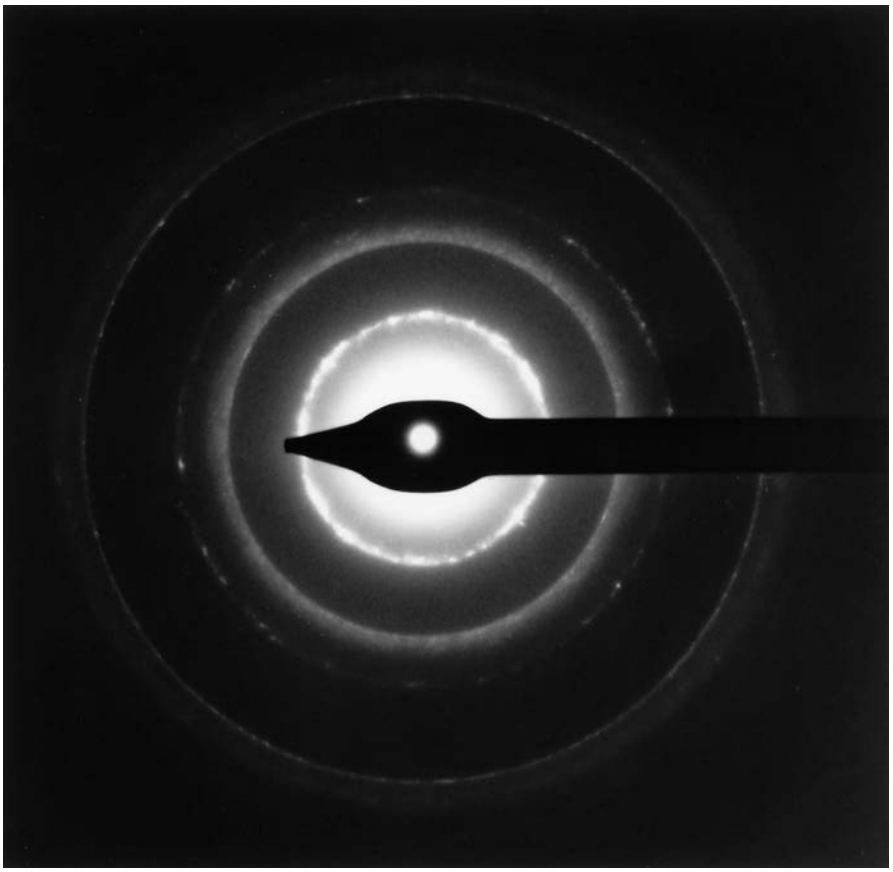

Fig. 6. Electron diffraction images of zirconium selenide particles. The evaluation of the diffraction rings does not correlate with any of the known zirconium selenide phases.

Table 2 Evaluation results of the diffraction pattern of zirconium selenide

Electron diffraction			$ZrSe_2$ JCPDS data #3-1189 [19]			Zr_2Se_3 JCPDS data #22-1027 [22]			
d-value (nm)	Intesity	*hkl*	Intensity (%)	*d*-values (nm) as published	*d*-values (nm) 9% dilation of the *a*- and *c*-axes	*hkl*	Intensity (%)	*d*-values (nm) as published	*d*-values (nm) 8% dilation of the *a*- and *c*-axes
0 338	very strong	002	–	0 3095	0 338	004/101	–/20	0 312/0 314	0 338/0 339
0 209	strong	110	80	0 189	0 207	015/110	40/75	0 198/0 187	0 214/0 202
0 168	weak	004	–	0 154	0 169	017	16	0 156	0 168
0 122	strong	024	–	0 128	0 122	028	–	0 126	0 122
0 118	very weak	030	60	0 110	0 119	215	6	0 110	0 119
0 105	very weak	124	60	0 097	0 106	035/218		0 099/0 096	0 107/0 104

imental values. Looking at the first diffraction line of the (00*i*) type, one realizes experimentally the maximum intensity at 0.589 nm. This corresponds to the β SnS_2 structure. However, the diffraction line observed at 0.306 nm is not allowed for β SnS_2. This line is allowed for the ordered polytype of the β SnS_2 structure. From these observations, one may conclude that the nanoparticles synthesized within this study represent a structural transition from the β SnS_2 structure to its ordered polytype.

Things are different for the $ZrSe_2$ nanoparticles. This material has obviously a layered structure but the diffraction pattern, depicted in Fig. 6 does not fit any of the phases with layered structure, $ZrSe_2$ and Zr_2Se_3, published in the JCPDS files. The electron diffraction pattern indicates a broad distribution of the distances between the lattice planes. Assuming a dilated *c* axis of 0.676 nm instead of 0.619 nm, the diffraction pattern differs significantly from that published for the hexagonal $ZrSe_2$ [19]. The second zirconium selenium phase with layered structure is Zr_2Se_3 [22]. In this case, a dilation of the *c* axis from the JCPDS value 1.251 1.351 nm has to be assumed. Furthermore this di lation in the *c* axis does not help to fit the actual diffraction pattern with that published.

Assuming a dilation of about 8 or 9% in the van der Waals bond *c* axis may be reasonable. If a simi lar dilation is assumed also in the *a* direction, the diffraction pattern obtained with the nanosized par ticles fit relatively well with the published diffrac tion pattern for $ZrSe_2$ or Zr_2Se_3. Certainly, this may not be a valid description of the actual struc ture, because dilating in the *a* direction means a dilation of the covalent bonds. Table 2 summarizes the results of measured *d* values and shows the possible calculated indices, based on a dilation of the *a* and *c* axes.

3.3. Compounds with C7 structure, disulphides and diselenides of molybdenum and tungsten

Figure 7 depicts the typical morphology of the MoS_2 particles synthesized in the 2.45 GHz equip ment. The size of these particles is in the range from 5 to 8 nm with a mean value of around 6 nm. Remarkably, in this case and in the case of WS_2, most of the particles consist of flat lattice planes with varying distances. The mean value of the dis tance between these layers, the {0002} planes, is 0.65 ± 0.07 nm, which has to be compared with a value of 0.6155 nm in a stoichiometric equilibrium crystal with sizes in the micrometre range [23]. Additionally, a few particles with bent lattice planes can be found. In contrast, the lattice parameters determined by electron diffraction, *a* 0.31 m and *c* 1.24 nm, correspond well with the powder dif fraction data (*a* 0.316 nm and *c* 1.22985 nm). Changing the experimental conditions to

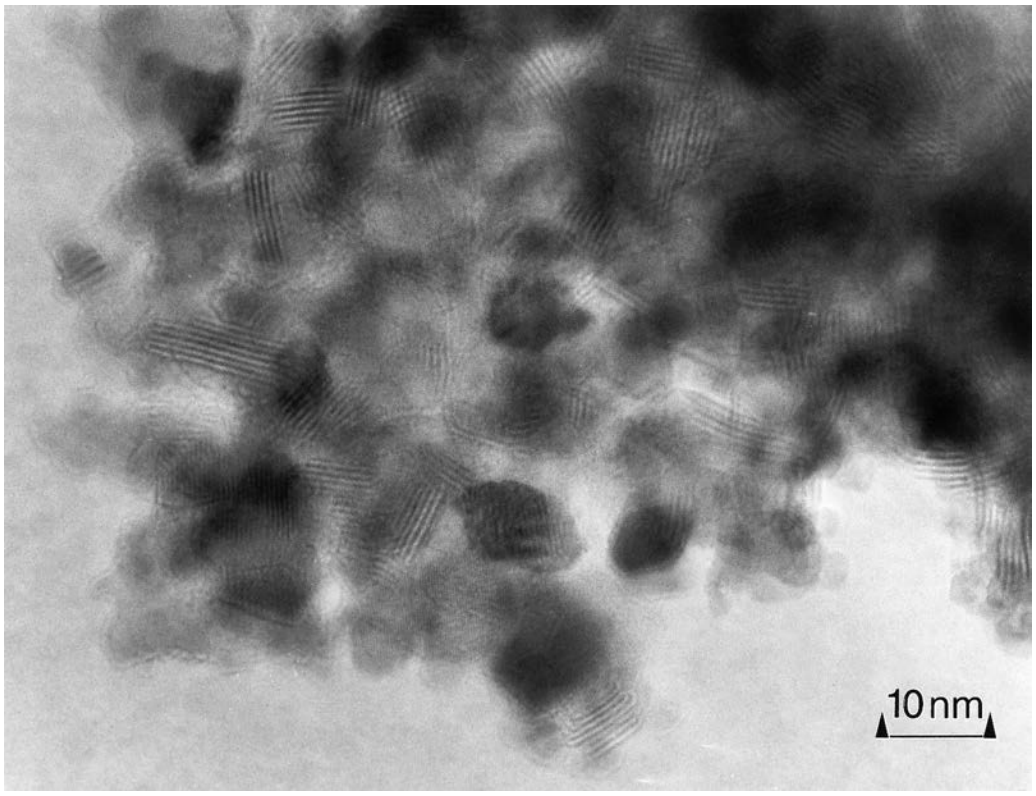

Fig. 7. Morphology of MoS_2 particles synthesized in the 2.45 GHz equipment at a temperature of 260°C. The lattice fringes represent the S Mo S layers, the {0002} planes with a measured distance of 0.65 nm.

0.915 GHz and a pressure of 30 mbar does not change the reaction product significantly. The main difference is the occurrence of particles with nested structures. Most of these particles show some extreme irregular shapes as shown in Fig. 8. There is a high probability, that these particles are not closed in three dimensions. Similar nested fullerene like particles were shown by Margulis *et al.* [2]. A typical example for a polyhedron like crystal is shown in Fig. 9. The particle depicted in this figure consists of three or four S Mo S triple planes, forming a box with rectangular cross section. The surface of this body is bent convexly. Figure 9(a) shows this particle under focus conditions where only the bent layers forming the walls (distance of the planes: 0.64 nm) can be seen. This bending leads to angles between the side walls that are not 90°. The Fourier power spectrum shown in this figure reveals a broad distribution of distances between the {0002} planes. Changing the imaging con ditions, one realizes additionally the lattice fringes of the bottom or top plane [Fig. 9(b)]. The distance of these lattice fringes is measured to be 0.23 nm and may belong to the $\{10\bar{1}3\}$ planes. The power spectrum reveals two striking phenomena. (i) The spacing in the ⟨0001⟩ direction is not constant within the different faces of the particle. One rather sees these spots radially elongated. (ii) The faces of the particle are not rectangular to each other. The deviation from 90° is at least 10°. Similar hollow polyhedra were described by Boulanger *et al.* [4] in the case of BN.

Relatively small and uniform WS_2 particles are obtained at a temperature of 160°C in a 2.45 GHz equipment (Fig. 10). The mean size of the particles is 5 nm. Typically, these particles show slightly bent lattice planes with a lattice spacing of 0.65 nm in the ⟨0001⟩ direction. Similar to the case of MoS_2 this value is significantly larger than the literature value [24] of 0.618 nm. The lattice parameters deter mined by electron diffraction (a 0.314 nm and c 1.24 nm) agree with the values indicated in the lit erature (a 0.3154 nm, c 1.2362 nm). As shown in Fig. 11, some particles show dislocation like structures. Nested fullerene like structures are not observed. Synthesizing this material in a 0.915 GHz plasma at a temperature of 260°C increases the size of the particles. Further increasing the temperature to 580°C leads to the occurrence of fullerene like particles (Fig. 12). The particle shown in this micro graph stems from a larger cluster. Therefore, lattice fringes from other particles are also visible. It was not possible to obtain a micrograph depicting the roof or the bottom of such a particle. Therefore, it is not proven that this particle is really a spherical one and not a bent two dimensional structure.

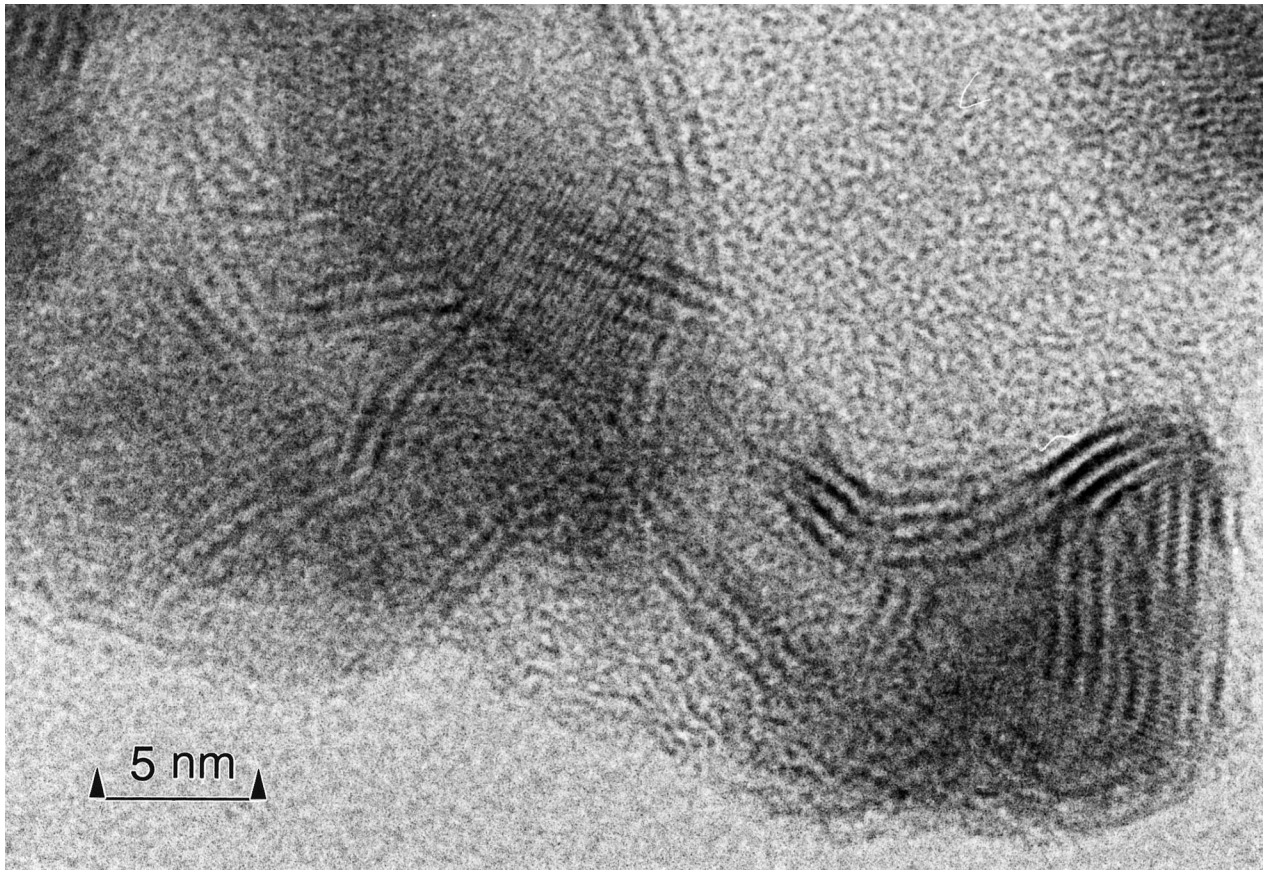

Fig. 8. Irregularly shaped non-equilibrium particles of MoS_2 (915 MHz, 260°C). There is a high probability that these nested particles are not closed in three dimensions.

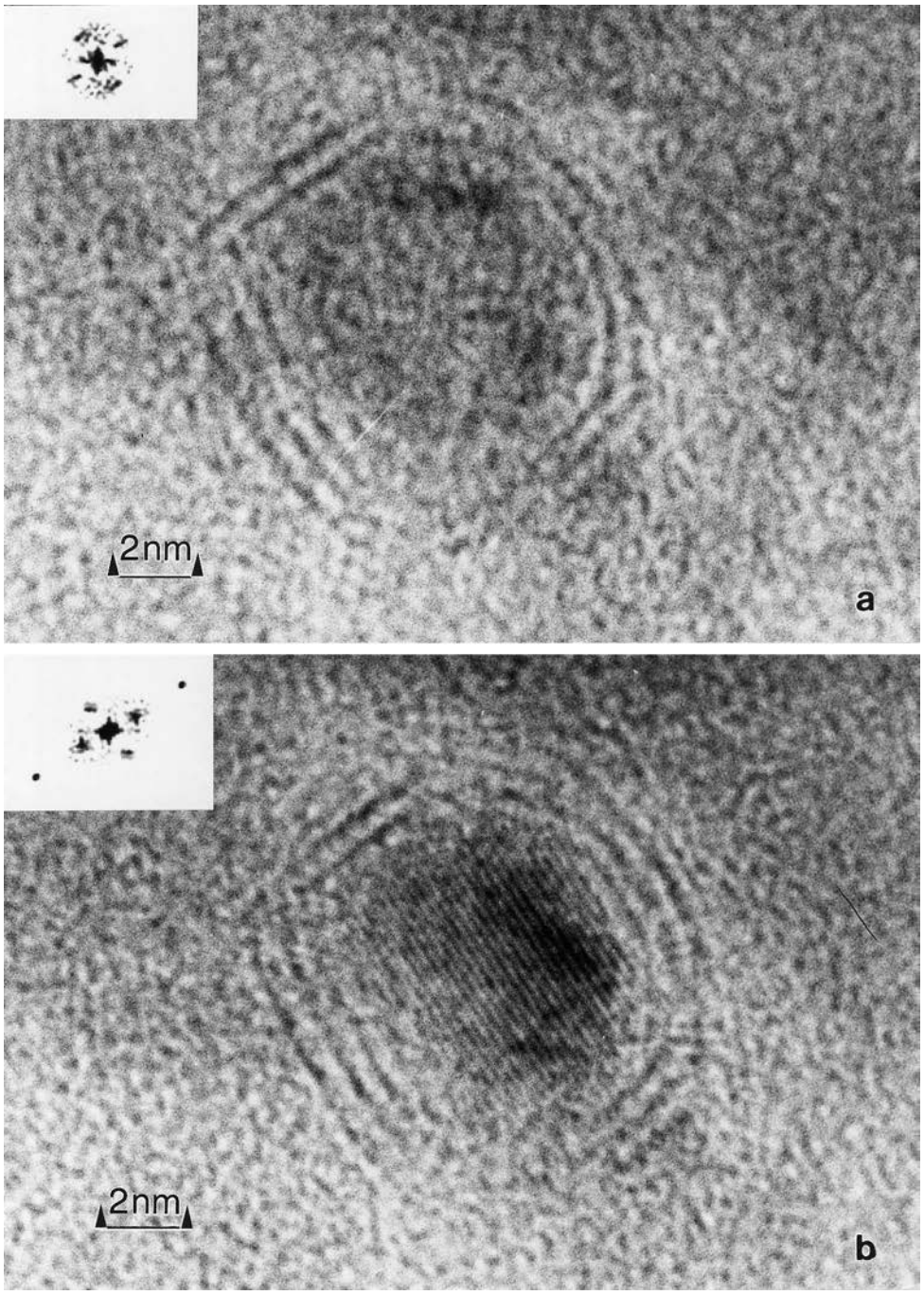

Fig. 9. Polyhedron shaped particle synthesized at 0.915 GHz and 260°C. This particle consisting of three or four S Mo S triple planes forms a box with convexly bent side walls. (a) Micrograph showing the side walls of the particle. The distance of the planes is measured to be 0.64 nm. The inset shows the central part of the power spectrum representing the lattice fringes. The relatively broad radial distribution of the spots representing the {0002} planes reveals strains in the ⟨0001⟩ direction. (b) Micrograph showing the side walls and the bottom or the roof of the particle depicted in (a). The distance of the additional lattice fringes is measured to be 0.23 nm. The power spectrum represents the lattice fringes of the {0002} and the $\{10\bar{1}3\}$ planes. Again, the relatively broad radial distribution of the spots representing the {0002} planes reveal strains in the ⟨0001⟩ direction.

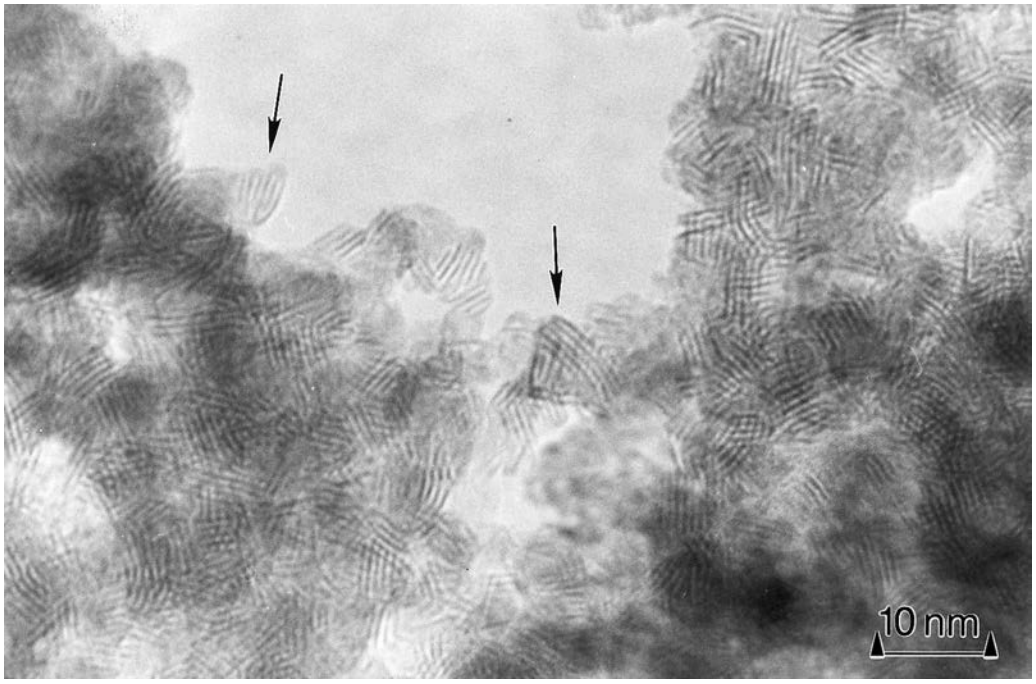

Fig. 10. Typical appearance of WS_2 particles synthesized at 2.45 GHz and 160°C. These particles show slightly bent lattice planes and some exhibit dislocation like structures (arrows).

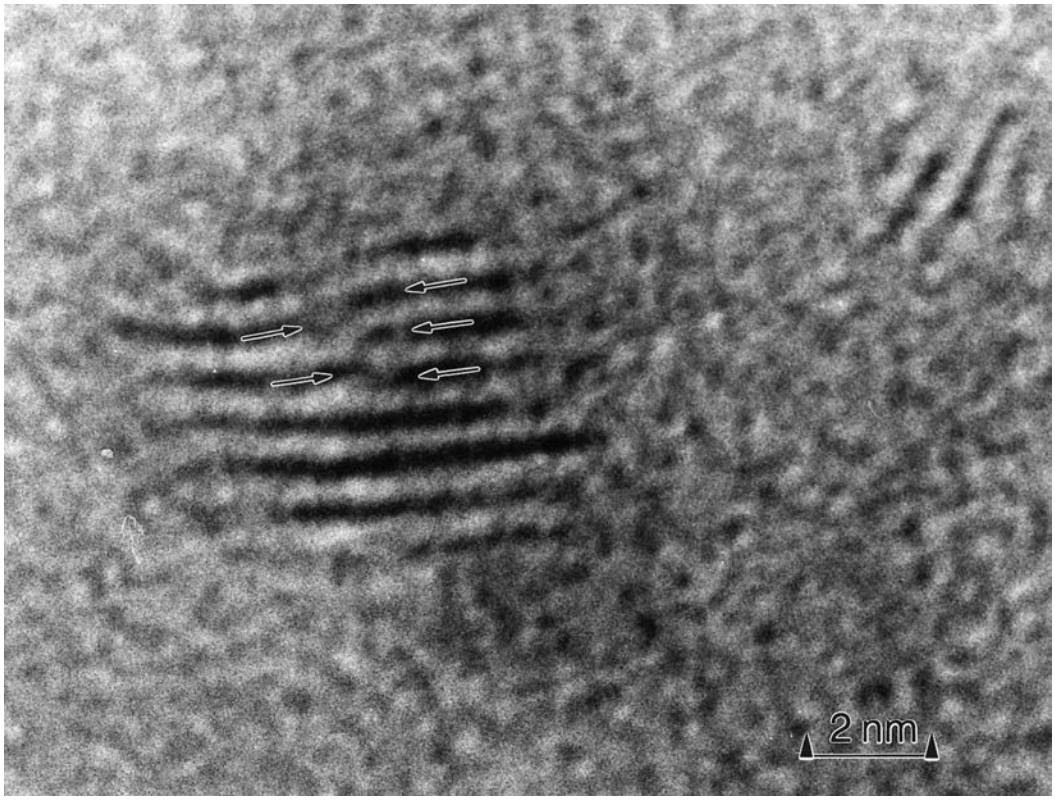

Fig. 11. A WS_2 particle of about 4 nm with a dislocation in the {0002} planes (synthesis conditions: 2.45 GHz, 160°C).

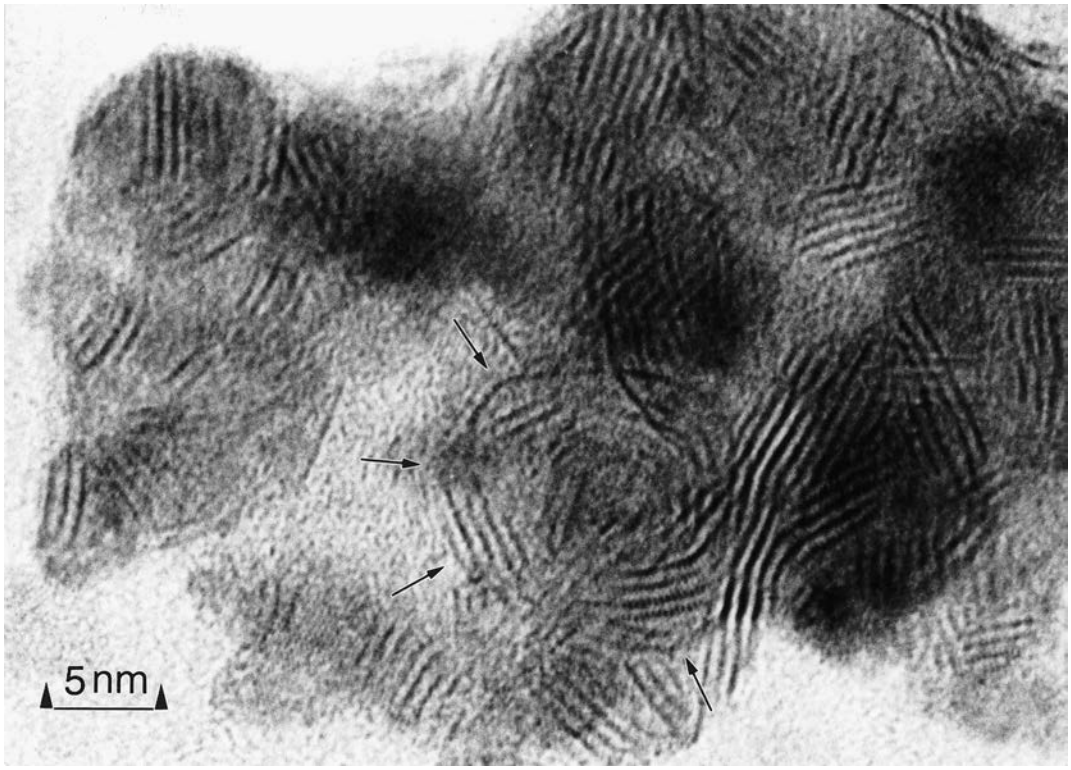

Fig. 12. Spherical WS_2 particle (arrows) synthesized at 0.915 GHz and 580°C.

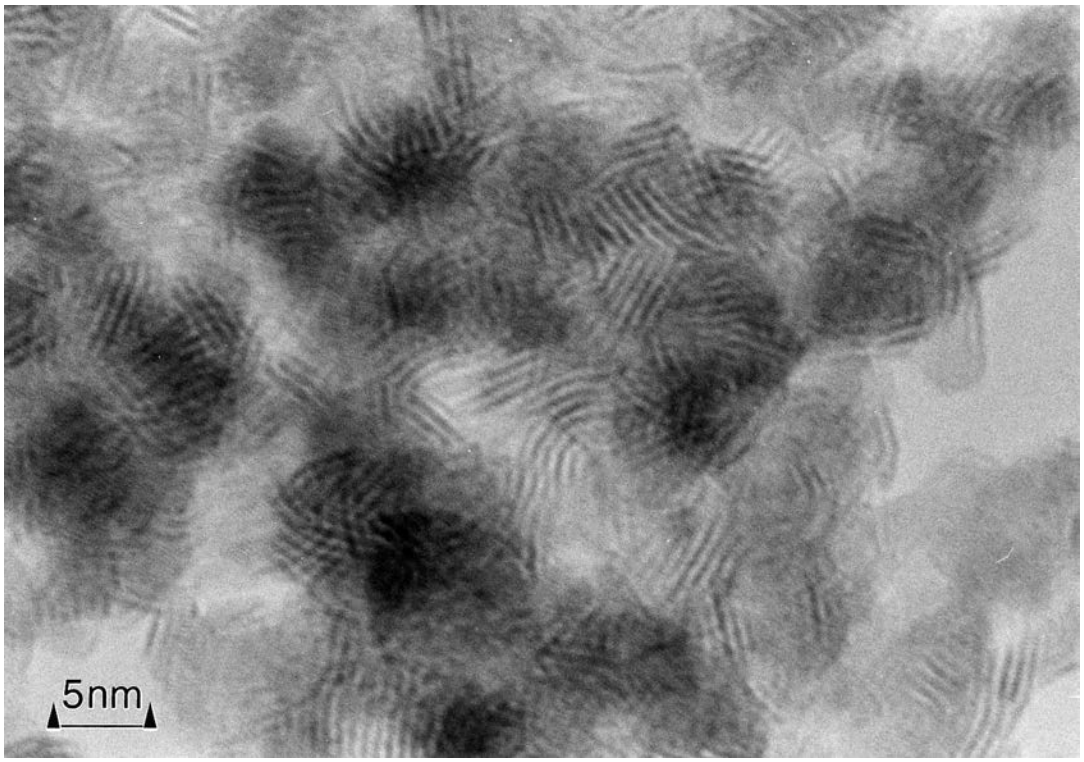

Fig. 13. $MoSe_2$ particles produced at 0.915 GHz and 500°C. The morphology of the $MoSe_2$ particles is very similar to MoS_2 particles.

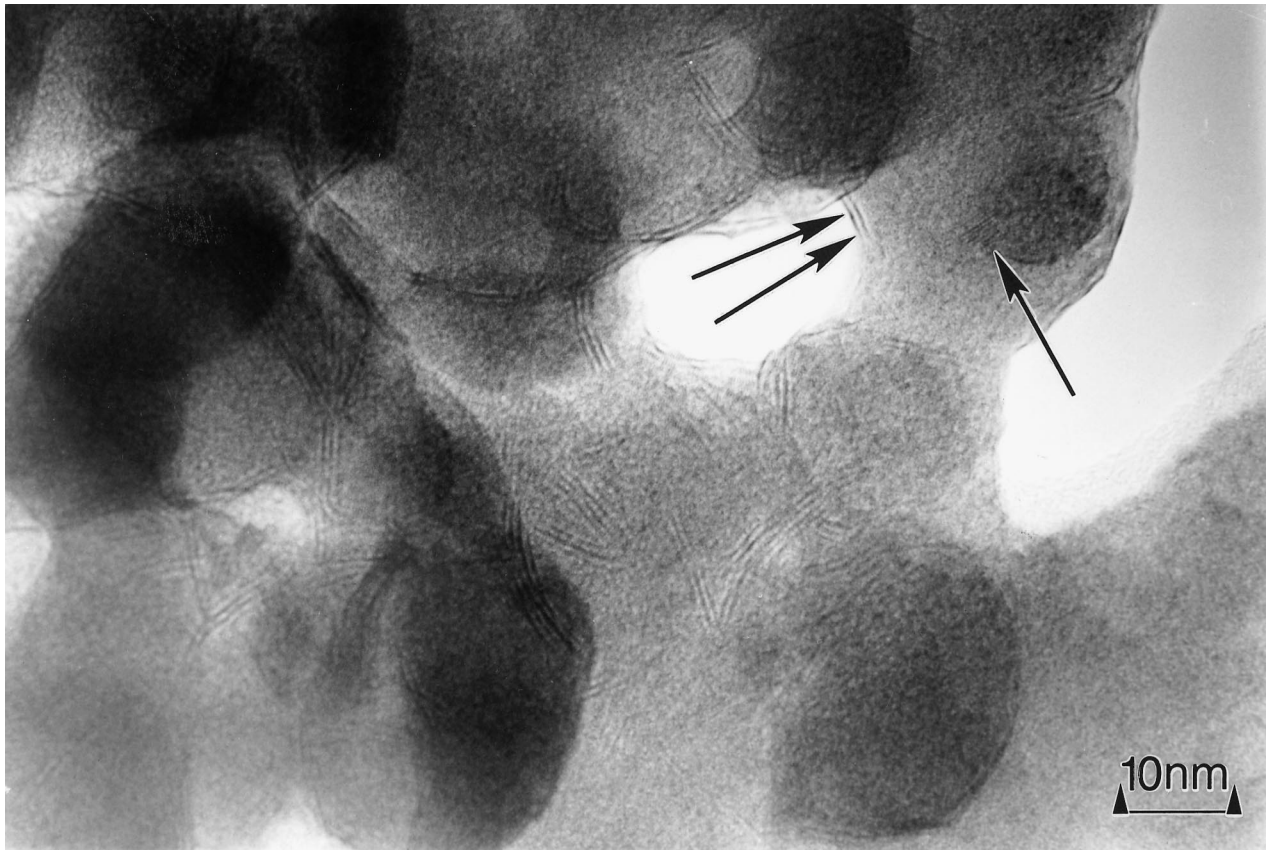

Fig. 14. Typical morphology of WSe_2 particles produced at 0.915 GHz and 500°C. The primary particles are amorphous and contain small crystallites (single arrow). During observation in the electron microscope, the crystallization of the amorphous particles into layered structures starts from the periphery (see double arrow).

Compatible with the fact that this particle has no edges, the power spectrum shows no deformation in any orientation.

The selenides of molybdenum and tungsten crystallize in the same structure but the appearance of the particles is entirely different. The morphology of $MoSe_2$ nanoparticles is comparable with that of the sulphide. Figure 13 depicts a typical example. The distance between the layers of $MoSe_2$ is 0.59 nm, corresponding to the {0002} layers. This is significantly smaller than the standard value of 0.646 nm indicated in the JPCD files [25]. By electron diffraction the distance of these layers is measured with 0.60 nm, whereas the lattice parameter in the *a* direction is not compressed. As already mentioned in Section 1, this is a general finding in layered compounds that was earlier found in MoS_2, WS_2 [1, 2, 5, 6, 9], and carbon [10].

In contrast, WSe_2 particles are, in general, not crystallized. Some of these glassy particles with sizes in the range from 20 to 30 nm show small crystallized inclusions with a size of about 5 nm. Heating these glassy particles with the electron beam in the electron microscope leads to another type of crystallization. As shown in Fig. 14, in this case the crystallization starts at the periphery of the particles forming bent layers. The particles depicted in this micrograph have formed about three to four crystallized layers.

4. CONCLUSIONS

For nanoparticles of compounds crystallizing in layered structures intuitively one expects either normal layered crystals or closed structures minimizing the number of dangling bonds at the periphery of the lattice planes. The latter assumption leads to fullerene like onion crystals, tubes, or polyhedron shaped closed aggregates. Assuming defects stemming from metal ions with varying valency, one may obtain particles with three dimensionally bent planes or in special cases step dislocations. Reality is more complex. All these phenomena were found in the examples crystallizing in the B8 (NiAs) and C7 (MoS_2) type structures. In these cases, deviations of the lattice spacing perpendicular to the layers from the values found on the specimen with sizes in the micrometre range were observed. Although the C6 (PbJ) structure is extremely similar to the C7 structure, $ZrSe_2$ and SnS_2 showed an entirely different morphology. These two compounds crystallized in rope like structures and not platelets or shapes derived from platelets. The reason for this different behaviour was not clear. Additionally, the diffraction pattern obtained from these compounds did not fit with that published in the JPCD files. From the analysis of the morphology of these structures, one may conclude the general rule that nanoparticles of compounds crystallizing in layered structures tend to form closed shapes. The formation of closed shapes reduces the number of dangling bonds on the periphery of the layers.

REFERENCES

1. Tenne, R., Margulis, L., Genut, M. and Hodes, G., *Nature*, 1992, **360**, 444.
2. Margulis, L., Saltra, G., Tenne, R. and Tallanker, M., *Nature*, 1993, **365**, 113.
3. José Yacamán, M., López, H., Santiago, P., Galván, D. H., Garzón, I. L. and Reyes, A., *Appl. Phys. Lett.*, 1996, **69**, 1065.
4. Boulanger, L., Andriot, B., Cauchetier, M. and Willaime, F., *Chem. Phys. Lett.*, 1995, **234**, 227.
5. Feldman, Y., Wasserman, E., Srolovitz, D. J. and Tenne, R., *Science*, 1995, **267**, 222.
6. Parilla, P. A., Dillon, A. C., Jones, K. M., Riker, G., Schulz, D. L., Ginley, D. S. and Heben, M. J., *Nature*, 1999, **397**, 114.
7. Luce, M., Croix, O., Zhou, Y. D., Cauchetier, M., Sapin, M. and Boulanger, M., in *Euroceramics II*, ed. G. Ziegler and H. Hausner. German Ceramic Society, Cologne, 1993, p. 233.
8. Baraton, M. I., Boulanger, M., Cauchetier, M., Lorenzelli, M., Luce, M., Merle, T., Quintard, T. and Zhou, Y., *J. Eur. Ceram. Soc.*, 1994, **13**, 372.
9. Feldman, Y., Frey, G. L., Homyonfer, M., Lyakhovitskaya, V., Margulis, L., Cohen, H., Hodes, G., Hutchinson, J. L. and Tenne, R., *J. Am. chem. Soc.*, 1996, **118**, 5362.
10. Banhart, F., Fuller, T., Redlich, Ph. and Ajayan, P. M., *Chem. Phys. Lett.*, 1997, **269**, 349.
11. Vollath, D. and Sickafus, K. E., *Nanostruct. Mater.*, 1992, **1**, 427.
12. Vollath, D. and Sickafus, K. E., *Nanostruct. Mater.*, 1993, **2**, 451.
13. Vollath, D., Seith, B. and Szabó, D. V., German Patent application P 196 28 357.4, 1996.
14. Vollath, D. and Mobius, A., First World Congress on Microwave Processing, Florida, 1997, paper XVII 4.
15. Hawkes, P. W., *Computer Processing of Electron Microscope Images*. Springer Verlag, Berlin, 1980.
16. Urban, J., Sack Kongehl, H. and Weiss, K., *Z. Physik D*, 1996, **36**, 73.
17. *NBS Monogr.*, 1983, **20**, 22 (JCPDS #34 421).
18. Golberg, D., Bando, Y., Stéphan, O. and Kurashima, K., *Appl. Phys. Lett.*, 1998, **73**, 2441.
19. van Arkel, A. E., *Physica*, 1924, **4**, 300, (JCPDS #3 1189).
20. *NBS Monogr.*, 1971, **9**, 25 (JCPDS #23 677).
21. Guenter, J. R. and Oswald, H. R., *Naturwiss.*, 1968, **55**, 177, (JCPDS #21 1231).
22. Salomons, W. and Wiegers, G. A., *Recl. Trav. Chim.*, 1968, **87**, 1339, (JCPDS #22 1027).
23. McMurdie, H. F., *et al.*, *Powder Diffract. J.*, 1986, **1**, 269, (JCPDS #37 1492).
24. *NBS Circular*, 1958, **8**, 539 (JCPDS #8 237).
25. Cech, F., Rieder, M. and Vrana, S., *Neues Jb. Miner. Mh.*, 1973, 433 (JCPDS #29 914).